Performance of synchronous optical receivers using atmospheric compensation techniques

Aniceto Belmonte[1,2] and Joseph M. Kahn[2]

[1.]*Technical University of Catalonia, Department of Signal Theory and Communications, 08034 Barcelona, Spain*
[2.] *Stanford University, Department of Electrical Engineering, Stanford, CA 94305, USA*
belmonte@tsc.upc.edu

Abstract: We model the impact of atmospheric turbulence-induced phase and amplitude fluctuations on free-space optical links using synchronous detection. We derive exact expressions for the probability density function of the signal-to-noise ratio in the presence of turbulence. We consider the effects of log-normal amplitude fluctuations and Gaussian phase fluctuations, in addition to local oscillator shot noise, for both passive receivers and those employing active modal compensation of wave-front phase distortion. We compute error probabilities for *M*-ary phase-shift keying, and evaluate the impact of various parameters, including the ratio of receiver aperture diameter to the wave-front coherence diameter, and the number of modes compensated.

© 2008 Optical Society of America

OCIS codes: (010.1330) Atmospheric turbulence; (030.6600) Statistical optics; (010.1080) Adaptive optics; (060.4510) Optical communications; (010.3640) Lidar.

References and links

1. D. L. Fried, "Optical heterodyne detection of an atmospherically distorted signal wave front," Proc. IEEE **55**, 57-67 (1967).
2. D. L. Fried, "Atmospheric modulation noise in an optical heterodyne receiver," IEEE J. Quantum Electron. **QE-3**, 213-221 (1967).
3. J. H. Churnside and C. M. McIntyre, "Signal current probability distribution for optical heterodyne receivers in the turbulent atmosphere. 1: Theory," Appl. Opt. **17**, 2141-2147 (1978).
4. J. H. Churnside and C. M. McIntyre, "Heterodyne receivers for atmospheric optical communications," Appl. Opt. **19**, 582-590 (1980).
5. K. A. Winick, "Atmospheric turbulence-induced signal fades on optical heterodyne communication links," Appl. Opt. **25**, 1817-1825 (1986).
6. N. Perlot, "Turbulence-induced fading probability in coherent optical communication through the atmosphere," Appl. Opt. **46**, 7218-7226 (2007).
7. A. Belmonte, "Influence of atmospheric phase compensation on optical heterodyne power measurements," Opt. Express **16**, 6756-6767 (2008).
8. E. Ip, A. P. T. Lau, D. J. F. Barros, and J. M. Kahn, "Coherent detection in optical fiber systems," Opt. Express **16**, 753-791 (2008).
9. M. P. Cagigal and V. F. Canales, "Speckle statistics in partially corrected wave fronts," Opt. Lett. **23**, 1072-1074 (1998).
10. J. W. Goodman, *Speckle Phenomena in Optics. Theory and Applications* (Ben Roberts & Company, 2007).
11. R. J. Noll, "Zernike polynomials and atmospheric turbulence," J. Opt. Soc. Am. **66**, 207-211 (1976).
12. M. Born and E. Wolf, *Principles of Optics* (Cambridge University Press, 1999)
13. J. W. Strohbehn, T. Wang, and J. P. Speck, "On the probability distribution of line-of-sight fluctuations of optical signals," Radio Science **10**, 59-70 (1975).
14. R. F. Pawula, S. O. Rice, and J. H. Roberts, "Distribution of the phase angle between two vectors perturbed by Gaussian noise," IEEE Trans. Commun. **COM-30**, 1828-1841 (1982).
15. L. C. Andrews, R. L. Phillips, and C. Y. Hopen, *Laser Beam Scintillation with Applications* (SPIE Press, 2001).

1. Introduction

Evaluating the performance of a heterodyne or homodyne receiver in the presence of atmospheric turbulence is generally difficult because of the complex ways turbulence affects the coherence of the received signal that is to be mixed with the local oscillator. The

downconverted heterodyne or homodyne power is maximized when the spatial field of the received signal matches that of the local oscillator. Any mismatch of the amplitudes and phases of the two fields will result in a loss in downconverted power. Adaptive compensation of atmospheric wave-front phase distortion to improve the performance of atmospheric systems has been an important field of study for many years. In particular, modal compensation method involves correction of several modes of an expansion of the total phase distortion in a set of basis functions.

Here, we study in a unified framework the effects of both wavefront distortion and amplitude scintillation on the performance of synchronous (coherent) receivers utilizing wavefront compensation. The effects ascribed to turbulence are random and subsequently must be described in a statistical sense. Early works quantified turbulence-induced fading through its mean and variance [1,2], although these are not adequate to fully characterize system performance. Later analyses have attempted to overcome these limitations and fully characterize the statistics of heterodyne optical systems by assuming a highly simplified model of atmospheric effects [3,4]. An alternate approach, aimed at overcoming the limitations of previous work, is based on numerical simulation of heterodyne optical systems [5,6]. Unfortunately, none of these prior works have resulted in an accurate statistical description of the performance of phase-compensated homodyne or heterodyne systems. Recently, a full-wave simulation of beam propagation has been used to examine the uncertainty inherent to the process of optical power measurement with a practical heterodyne receiver because of the presence of refractive turbulence [7].

The remainder of this paper is organized as follows. In Section 2, we define a mathematical model for the received signal after propagation through the atmosphere. By noting that the downconverted signal current can be characterized as the sum of many contributions from different coherent regions within the aperture, we show that the probability density function (PDF) of this current can be well-approximated by a modified Rice distribution. In our model, the parameters describing the PDF depend on the turbulence conditions and the degree of modal compensation applied in the receiver. In Section 3, we compute the error probability for QPSK modulation in the presence of multiplicative noise from atmospheric turbulence and additive white Gaussian noise (AWGN). We provide analytical expressions for the error probability of synchronous communication systems, and use them to study the effect of various parameters on performance, including turbulence level, signal strength, receive aperture size, and the extent of wavefront compensation.

2. First-order statistics in optical homodyne or heterodyne detection

When a received signal experiences atmospheric turbulence during transmission, both its envelope and its phase fluctuate over time. In the case of coherent modulation, phase fluctuations can severely degrade performance unless measures are taken to compensate for them at the receiver. Here, we assume that after homodyne or heterodyne downconversion is used to obtain an electrical signal, the receiver is able to track any phase fluctuations caused by turbulence (as well as those caused by laser phase noise), performing ideal coherent (synchronous) demodulation. Under this assumption, analyzing the receiver performance requires knowledge of only the envelope statistics of the downconverted electrical signal.

In a coherent receiver, downconversion from the optical domain to the electrical domain can be achieved using either heterodyne or homodyne methods [8]. The performance comparison between homodyne and heterodyne depends on the modulation scheme being considered. This paper analyzes QPSK modulation with synchronous homodyne or heterodyne detection, assuming the dominant noise is local oscillator shot noise. For concreteness, equations are given for the heterodyne case, but the signal-to-noise ratio (SNR) and error-rate performance are the same for the homodyne case. We assume the heterodyne downconverter uses a 50-50 beamsplitter and a pair of photodetectors, comprising a balanced receiver. (Using BPSK modulation, it is possible to employ a single-quadrature downconverter for homodyne but not heterodyne. Hence, for BPSK, homodyne can achieve a

given error rate at a 3-dB lower signal power than heterodyne in the shot-noise-limited regime.)

In order to assess the impact of turbulence, both log-amplitude and phase fluctuations should be considered. As a consequence, the field in the pupil plane is expressed as

$$A = A_S \exp\left[\chi(\boldsymbol{r}) - j\phi(\boldsymbol{r})\right], \tag{1}$$

where A_s is the amplitude without the effect of turbulence, and $\chi(\boldsymbol{r})$ and $\phi(\boldsymbol{r})$ represent the log-amplitude fluctuations (scintillation) and phase variations (aberrations), respectively, introduced by atmospheric turbulence. In the heterodyne downconverter, the information-carrying photocurrent i_s at the output of the balanced receiver is:

$$i_S = \eta A_0 A_S \int d\boldsymbol{x} \, W(\boldsymbol{r}) \exp\left[\chi(\boldsymbol{r})\right] \cos\left[2\pi \Delta f \, t + \Delta\phi - \phi(\boldsymbol{r})\right], \tag{2}$$

where η is the quantum efficiency of the photodetector, A_0 is the amplitude of the local oscillator, and Δf and $\Delta\phi$ are, respectively, the differences between the frequencies and phases of the signal and local oscillator. The circular receiving aperture of diameter D is defined by the aperture function $W(\boldsymbol{r})$, which equals unity for $|\boldsymbol{r}| \leq D/2$, and equals zero for $|\boldsymbol{r}| > D/2$. We can rewrite the cosine using $\cos(u - v) = \cos u \cos v + \sin u \sin v$, obtaining

$$i_S = \eta A_0 A_S \left\{ \cos\left[2\pi \Delta f \, t + \Delta\phi\right] \int d\boldsymbol{r} \, W(\boldsymbol{r}) \exp\left[\chi(\boldsymbol{r})\right] \cos\left[\phi(\boldsymbol{r})\right] + \right.$$
$$\left. + \sin\left[2\pi \Delta f \, t + \Delta\phi\right] \int d\boldsymbol{r} \, W(\boldsymbol{r}) \exp\left[\chi(\boldsymbol{r})\right] \sin\left[\phi(\boldsymbol{r})\right] \right\}. \tag{3}$$

Taking the time average of the beat frequency Δf oscillations of Eq. (3), the average detected signal power $\overline{i_S^2}$ may be written as

$$\overline{i_S^2} = \frac{1}{2}\left(\eta \frac{\pi}{4} D^2 A_0 A_S\right)^2 \left[\alpha_r^2 + \alpha_i^2\right], \tag{4}$$

where α_r and α_i are normalized versions of the integrals in Eq. (3):

$$\alpha_r = \left(\frac{\pi}{4} D^2\right)^{-1} \int d\boldsymbol{r} \, W(\boldsymbol{r}) \exp\left[\chi(\boldsymbol{r})\right] \cos\left[\phi(\boldsymbol{r})\right]$$
$$\alpha_i = \left(\frac{\pi}{4} D^2\right)^{-1} \int d\boldsymbol{r} \, W(\boldsymbol{r}) \exp\left[\chi(\boldsymbol{r})\right] \sin\left[\phi(\boldsymbol{r})\right]. \tag{5}$$

In this last step, the trigonometric and exponential terms have been considered time-independent, as the time average is taken over a period that is short compared with the coherence time associated with atmospheric turbulence. It is important to note that α_r and α_i represent integrals over the collecting aperture of the real and imaginary parts, respectively, of the normalized optical field reaching the receiver. These real and imaginary parts can be considered as the components of a complex random phasor.

If the noise is dominated by local oscillator shot noise, the average noise power per unit bandwidth is $\overline{i_N^2} = e\,\eta\,\pi/4\,D^2\,A_0^2$, where e is the electronic charge. The SNR per unit bandwidth $\gamma = \overline{i_S^2}/\overline{i_N^2}$ can be expressed using Eq. (4) as

$$\gamma = \frac{1}{2}\left(\frac{\eta}{e}\right) \frac{\pi}{4} D^2 A_S^2 \ \alpha^2. \tag{6}$$

Note that the SNR in the presence of turbulence, γ, is proportional to the SNR in the absence of turbulence, $\gamma_0 = \frac{1}{2}(\eta/e)\ \pi/4\,D^2\,A_S^2$:

$$\gamma = \gamma_0 \; \alpha^2 . \tag{7}$$

The constant of proportionality is $\alpha^2 = \alpha_r{}^2 + \alpha_i{}^2$, a random scale factor representing the effect of both the amplitude and phase fluctuations of the optical field. The statistical properties of the random variable α^2, with mean $\overline{\alpha^2}$ and PDF $p_{\alpha^2}(\alpha^2)$, provide a statistical characterization of the SNR γ. Using the average SNR $\overline{\gamma} = \gamma_0 \overline{\alpha^2}$ and the Jacobian of the transformation $\alpha^2 = \gamma/\gamma_0 = \gamma \overline{\alpha^2}/\overline{\gamma}$, we obtain the PDF of the SNR:

$$p_\gamma(\gamma) = \frac{\overline{\alpha^2}}{\overline{\gamma}} \, p_{\alpha^2}\left(\gamma \; \frac{\overline{\alpha^2}}{\overline{\gamma}} \right) . \tag{8}$$

Turning attention to α^2, we study how amplitude and phase fluctuations of the optical field define the statistics of the fading intensity $\alpha^2 = \alpha_r{}^2 + \alpha_i{}^2$. We note that the two random magnitudes α_r and α_i are expressed in Eq. (5) as integrals over the aperture and, hence, are the sums of contributions from each point in the aperture. In order to proceed with the analysis, we consider a statistical model in which these continuous integrals are expressed as finite sums over N statistically independent cells in the aperture:

$$\alpha_r \cong \frac{1}{N} \sum_{k=1}^{N} \exp \chi_k \cos \phi_k$$
$$\alpha_i \cong \frac{1}{N} \sum_{k=1}^{N} \exp \chi_k \sin \phi_k \; , \tag{9}$$

where χ_k is the log-amplitude and ϕ_k is the phase of the kth statistically independent cell. A similar approach has been used to analyze the statistics of the Strehl ratio [9]. The mean log-amplitude can be extracted out of the sums, yielding

$$\alpha_r \cong \frac{1}{N} \exp \overline{\chi} \sum_{k=1}^{N} \exp(\chi_k - \overline{\chi}) \cos \phi_k$$
$$\alpha_i \cong \frac{1}{N} \exp \overline{\chi} \sum_{k=1}^{N} \exp(\chi_k - \overline{\chi}) \sin \phi_k \; . \tag{10}$$

Under the assumption that N, the number of independent cells, is large enough, we can consider that α_r and α_i asymptotically approach jointly normal random variables:

$$p_{\alpha_r,\alpha_i}(\alpha_r,\alpha_i) = \frac{1}{2\pi\sigma_r\sigma_i} \exp\left[-\frac{(\alpha_r - \overline{\alpha}_r)^2}{2\sigma_r^2} \right] \exp\left[-\frac{(\alpha_i - \overline{\alpha}_i)^2}{2\sigma_i^2} \right], \tag{11}$$

where $\overline{\alpha}_r$, $\overline{\alpha}_i$ and σ_r^2, σ_i^2 are the means and variances of α_r, α_i, which are required to evaluate the joint PDF. To estimate these means and variances, we recall that α_r and α_i can be considered as the real and imaginary parts of a random phasor. Hence, it is possible to evaluate the means and variances of α_r and α_i by using the classical statistical model for speckle with a non-uniform distribution of phases [10]. After some algebraic manipulation, mean values can be obtained as

$$\overline{\alpha}_r = \frac{1}{2} \exp \overline{\chi} \; \overline{\exp(\chi_k - \overline{\chi})} \left[M_\phi(1) + M_\phi(-1) \right]$$
$$\overline{\alpha}_i = -\frac{j}{2} \exp \overline{\chi} \; \overline{\exp(\chi_k - \overline{\chi})} \left[M_\phi(1) - M_\phi(-1) \right], \tag{12}$$

and the variances are given by

$$\sigma_r^2 = \frac{\exp 2\overline{\chi}\ \overline{\exp 2(\chi_k - \overline{\chi})}}{4N}\left[2 + M_\phi(2) + M_\phi(-2)\right]$$

$$-\frac{\exp 2\overline{\chi}\left[\overline{\exp(\chi_k - \overline{\chi})}\right]^2}{4N}\left[2M_\phi(1)M_\phi(-1) + M_\phi^2(1) + M_\phi^2(-1)\right],$$

$$\sigma_i^2 = \frac{\exp 2\overline{\chi}\ \overline{\exp 2(\chi_k - \overline{\chi})}}{4N}\left[2 - M_\phi(2) - M_\phi(-2)\right]$$

$$-\frac{\exp 2\overline{\chi}\left[\overline{\exp(\chi_k - \overline{\chi})}\right]^2}{4N}\left[2M_\phi(1)M_\phi(-1) - M_\phi^2(1) - M_\phi^2(-1)\right]. \tag{13}$$

$M_\phi(\omega)$ is the characteristic function of the phase, i.e., the Fourier transform of its PDF . We point out that because α_r, α_i result from atmospheric turbulence, we can consider phases ϕ_k that obey zero-mean Gaussian statistics: $p_\phi(\phi) = 1/\sqrt{2\pi}\sigma_\phi \exp(-\phi^2/2\sigma_\phi^2)$. In this case, the characteristic function of the phase is:

$$M_\phi(\omega) = \exp\left(-\frac{\sigma_\phi^2 \omega^2}{2}\right). \tag{14}$$

In [11], the statistics of phase aberrations caused by atmospheric turbulence were characterized, considering a Kolmogorov spectrum of turbulence. In that analysis, classical results for the phase variance σ_ϕ^2 were extended to consider modal compensation of atmospheric phase distortion. In such modal compensation, Zernike polynomials are widely used as basis functions because of their simple analytical expressions and their correspondence to classical aberrations [12]. It is known that the residual phase variance after modal compensation of J Zernike terms is given by

$$\sigma_\phi^2 = C_J\left(\frac{D}{r_0}\right)^{5/3}, \tag{15}$$

where the aperture diameter D is normalized by the wavefront coherence diameter r_0, which describes the spatial correlation of phase fluctuations in the receiver plane [1]. In (15), the coefficient C_J depends on J [11]. For example, aberrations up to tilt, astigmatism, coma and fifth-order correspond to $J = 3, 6, 10$ and 20, respectively. Ideally, it is desirable to choose J large enough that the residual variance Eq. (15) becomes negligible.

If it is also assumed that the log-amplitudes χ_k are normal random variables [13], we can use energy conservation, and the expressions for the mean of exponential functions of Gaussian variables, to obtain classical results for the log-amplitude and amplitude means:

$$\overline{\chi} = -\sigma_\chi^2$$
$$\overline{\exp(\chi_k - \overline{\chi})} = \exp\left(\frac{1}{2}\sigma_\chi^2\right). \tag{16}$$

The irradiance $\beta \equiv \exp 2(\chi_k - \overline{\chi})$ has a mean given by $\exp(2\sigma_\chi^2)$. The log-amplitude variance σ_χ^2 is often expressed as a scintillation index $\sigma_\beta^2 = \exp(4\sigma_\chi^2) - 1$.

Substitution of Eq. (14) and Eq. (16) into Eq. (12) and Eq. (13) yields

$$\bar{\alpha}_r = \exp\left(-\frac{1}{2}\sigma_\chi^2\right)\exp\left(-\frac{1}{2}\sigma_\phi^2\right)$$

$$\bar{\alpha}_i = 0$$

$$\sigma_r^2 = \frac{1}{2N}\left[1+\exp\left(-2\sigma_\phi^2\right)-2\exp\left(-\sigma_\chi^2\right)\exp\left(-\sigma_\phi^2\right)\right]$$

$$\sigma_i^2 = \frac{1}{2N}\left[1-\exp\left(-2\sigma_\phi^2\right)\right].$$

(17)

At this point, we still need to determine the number of statistically independent patches or cells N present in the aperture. An analytical expression to estimate N can be defined by

$$N = \left[\frac{1}{S}\int d\boldsymbol{r}\ W(\boldsymbol{r})\ C(\boldsymbol{r})\right]^{-1},$$

(18)

where $W(\boldsymbol{r})$ again characterizes the collecting aperture with area $S = (\pi/4)D^2$. Here, $C(\boldsymbol{r})$ is the coherence function describing the wavefront distortion introduced by atmospheric turbulence [1]

$$C(\boldsymbol{r}) = \exp\left[-\frac{1}{2}6.88\left(\frac{r}{r_0}\right)^{5/3}\right].$$

(19)

Physical insight into Eq. (18) may be obtained by considering the limiting case in which the receiver aperture is much greater than the coherence diameter r_0, i.e., $D \gg r_0$. In this case,

$$N = \left[\frac{8}{D^2}\int_0^\infty r\,dr\ \exp\left[-\frac{1}{2}6.88\left(\frac{r}{r_0}\right)^{5/3}\right]\right]^{-1}.$$

(20)

The integral can be solved in a closed form to obtain $N = [1.007\ (r_0/D)^2]^{-1}$. To a good approximation, the aperture can be considered to consist of $(D/r_0)^2$ independent cells, each of diameter r_0. In the opposite extreme of an aperture much smaller than the coherence diameter, $D \ll r_0$, we have $C(\boldsymbol{r}) \approx 1$ and $N = 1$. This result indicates that as the aperture gets smaller, the number of cells approaches unity. Values of $N < 1$ are not possible. An analytical expression for N valid for all aperture diameters is given by

$$N = \left[\frac{8}{D^2}\int_0^{D/2} r\,dr\ \exp\left[-\frac{1}{2}6.88\left(\frac{r}{r_0}\right)^{5/3}\right]\right]^{-1},$$

(21)

which can easily be integrated to yield

$$N = \left\{1.09\left(\frac{r_0}{D}\right)^2\Gamma\left[\frac{6}{5},1.08\left(\frac{D}{r_0}\right)^{5/3}\right]\right\}^{-1}.$$

(22)

Here, $\Gamma(a,x)$ is the lower incomplete gamma function. Equation (22) will be used to estimate the value of N needed to evaluate Eq. (17).

Turning again to the distribution function of interest, a joint PDF of intensity α^2 and phase θ can be found by substituting $a_r = \sqrt{\alpha^2}\cos\theta$, $a_i = \sqrt{\alpha^2}\sin\theta$ into Eq. (11), and multiplying the resulting expression by the Jacobian of the transformation, $1/2$. To obtain the marginal PDF of the fading intensity α^2, we integrate with respect to θ:

$$p_{\alpha^2}\left(\alpha^2\right)=\frac{1}{4\pi}\frac{1}{\sigma_r\sigma_i}\int_{-\pi}^{\pi}d\theta\,\exp\left[-\frac{\left(\alpha\cos\theta-\bar{\alpha}_r\right)^2}{2\sigma_r^2}\right]\exp\left[-\frac{\left(\alpha\sin\theta\right)^2}{2\sigma_i^2}\right]. \tag{23}$$

Unfortunately, the integral in Eq. (23) cannot be performed in closed form. Since α_r and α_i are jointly normal random variables, it is possible to obtain the mean and variance of the intensity fading as $\overline{\alpha^2}=\sigma_r^2+\sigma_i^2+\overline{\alpha}_r^2$ and $\sigma_{\alpha^2}^2=2\left(\sigma_r^4+\sigma_i^4\right)+4\sigma_r^2\bar{\alpha}_r^2$. It is instructive to consider the weak-turbulence, near-field regime, where values of σ_ϕ^2 and σ_χ^2 are small but the log-amplitude variance σ_χ^2 can be neglected in comparison to the effect of phase aberrations. From Eq. (17), we obtain $\sigma_r^2=0$, $\bar{\alpha}_r=1-\sigma_\phi^2/2$, and $\sigma_i^2=\sigma_\phi^2/N$. In this case, the fading intensity α^2 is defined as the sum of a constant (coherent) term α_r with amplitude $\bar{\alpha}_r$ and a random (incoherent) term α_i with zero mean and variance σ_i^2. Such a random variable, defined as the sum of a known dominant phasor plus a random phasor sum, is characterized by a Rice PDF [10]:

$$p_{\alpha^2}\left(\alpha^2\right)=\frac{1}{2\sigma^2}\exp\left[-\frac{\alpha^2+a^2}{2\sigma^2}\right]I_0\left(\frac{a\alpha}{\sigma^2}\right), \tag{24}$$

where $a^2=\overline{\alpha}_r^2$ and $2\sigma^2=\sigma_i^2$. The parameter a^2 represents the coherent intensity that dominates over the fluctuating residual halo, whose intensity is represented by $2\sigma^2$. It is convenient to express the basic Rice PDF (24) in terms of the mean $\overline{\alpha^2}=2\sigma^2+a^2$ and the contrast parameter $1/r\equiv2\sigma^2/a^2$, a measure of the strength of the residual halo to the coherent component:

$$p_{\alpha^2}\left(\alpha^2\right)=\frac{1+r}{\overline{\alpha^2}}\exp\left(-r\right)\exp\left[-\frac{\left(1+r\right)\alpha^2}{\overline{\alpha^2}}\right]I_0\left(2\alpha\sqrt{\frac{\left(1+r\right)r}{\overline{\alpha^2}}}\right), \tag{25}$$

which is often referred to as the modified Rician PDF. The variance of the intensity fading $\sigma_{\alpha^2}^2$ can be expressed in terms of mean value $\overline{\alpha^2}$ and the parameter r as $\sigma_{\alpha^2}^2=\overline{\alpha^2}\left(2r+1\right)/\left(1+r\right)^2$.

It is possible to extend this convenient Rice distribution to stronger turbulence regimes, in which both the phase aberrations σ_ϕ^2 and the log-amplitude variance σ_χ^2 need to be considered. We can expect the general marginal PDF Eq. (23) to behave like the Rice PDF Eq. (25) provided that we can find a set of equivalent Rice parameters ($\overline{\alpha^2}$ and r) that makes Eq. (17) and Eq. (19) have identical mean and variance. Comparing the means and variances of the two distributions, the required values of $\overline{\alpha^2}$ and r can be computed as functions of $\bar{\alpha}_r$, σ_r^2, and σ_i^2 through the relations

$$\begin{aligned}\overline{\alpha^2}&=\sigma_r^2+\sigma_i^2+\bar{\alpha}_r^2\\\overline{\alpha^2}\left(2r+1\right)\big/\left(1+r\right)^2&=2\left(\sigma_r^4+\sigma_i^4\right)+4\sigma_r^2\bar{\alpha}_r^2.\end{aligned} \tag{26}$$

After some algebra, the contrast parameter $1/r$ can be obtained from Eq. (26) as

$$\frac{1}{r}=\frac{\sigma_r^2+\sigma_i^2+\overline{a}_r^2}{\left[\overline{a}_r^4+2\overline{a}_r^2\left(\sigma_i^2-\sigma_r^2\right)-\left(\sigma_i^2-\sigma_r^2\right)^2\right]^{1/2}}-1, \tag{27}$$

where the mean $\bar{\alpha}_r$ and variances σ_r^2, σ_r^2 are obtained with the help of Eq. (17).

We have just redefined the Rician model so the dominant component can be a phasor sum of two or more dominant waves, and can be subject to amplitude fluctuations (scintillation). The parameter r ranges between 0 and ∞. It can be shown that when the dominant term is very weak ($r\rightarrow0$), intensity fading α^2 becomes negative-exponential-distributed, just as in a speckle pattern. Likewise, when the dominant term is very strong ($r\rightarrow\infty$), the density function becomes highly peaked around the mean value $\overline{\alpha^2}$, and there is no fading to be considered. When r is large, it can be shown that the PDF of α^2 is, except for a skewness factor α, approximately Gaussian with mean $\overline{\alpha^2}$. Consequently, the Rice distribution can describe the entire range of fading that needs to be considered in our analysis.

Using Eq. (25) to express the PDF of the fading intensity α^2, and applying Eq. (8), we find that the SNR γ is described by a noncentral chi-square distribution with two degrees of freedom:

$$p_\gamma(\gamma) = \frac{1+r}{\overline{\gamma}}\exp(-r)\exp\left[-\frac{(1+r)\gamma}{\overline{\gamma}}\right]I_0\left[2\sqrt{\frac{(1+r)r\gamma}{\overline{\gamma}}}\right], \qquad (28)$$

where the mean SNR $\overline{\gamma} = \gamma_0\overline{\alpha^2}$ depends on turbulence-free SNR γ_0 and the parameter $\overline{\alpha^2}$ describing turbulence effects.

While we have a plausible model leading to the Rice and noncentral chi-square distributions, the choice of the beta distribution in [6] is based on a resemblance of the observed curves in some numerical simulations, and not on any statistical reasoning. It is not clear how the parameters of the beta distribution must be (heuristically) fitted. Also, it result difficult to extent those results to coherent optical receivers using atmospheric compensation techniques. The framework of our approach is mathematically more robust and leads to results easily extendable to systems employing active modal compensation.

3. Performance of coherent receivers

In the presence of turbulence, the received power is scaled by the fading intensity α^2, a random variable with PDF $p_{\alpha^2}(\alpha^2)$, which depends on atmospheric propagation. At the receiver, the signal is perturbed by AWGN, which is statistically independent of the fading intensity α^2. Hence, the instantaneous SNR γ is proportional to α^2. The symbol-error probability (SEP) $p_s(E)$ of an ideal coherent receiver is obtained by averaging the SEP conditioned on the SNR γ over the PDF of the instantaneous SNR, $p_\gamma(\gamma)$:

$$p_S(E) = \int_0^\infty d\gamma\, p_S(E\,|\,\gamma)\, p_\gamma(\gamma). \qquad (29)$$

Although our model can accommodate various modulation/detection schemes, in this paper, we consider M-ary phase-shift keying (M-PSK) with ideal coherent detection based on maximum-likelihood principles. In this case, the SEP conditioned on the instantaneous SNR is given by [14]

$$p_S(E\,|\,\gamma) = \int_{-\pi/2}^{\pi/2-\pi/M} d\theta\, \exp\left(-\gamma\frac{\sin^2\frac{\pi}{M}}{\sin^2\theta}\right). \qquad (30)$$

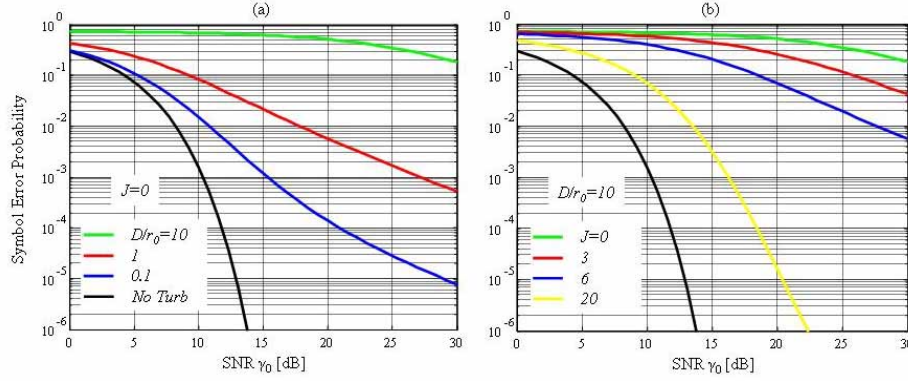Using Eqs. (30) and (28) in Eq. (29), after some algebra, we obtain

Fig. 1. Symbol-error probability (SEP) vs. turbulence-free SNR per symbol γ_0 for QPSK with coherent detection and additive white Gaussian noise (AWGN). Performance is shown for different values of: (a) the normalized receiver aperture diameter D/r_0, and (b) the number of modes J removed by adaptive optics. Amplitude fluctuations are neglected by assuming $\sigma_\beta^2=0$. Turbulence is characterized by the phase coherence length r_0. In (a), D/r_0 ranges from 0.1 (weak turbulence) to 10 (strong turbulence). In (b), the compensating phases are expansions up to tilt ($J=3$), astigmatism ($J=6$), and 5th-order aberrations ($J=20$). The no-correction case ($J=0$) is also considered. The no-turbulence case is indicated by black lines.

$$p_S\left(E\right)=\frac{1}{\pi}\int_{-\pi/2}^{\pi/2-\pi/M}d\theta\ \frac{\left(1+r\right)\sin^2\theta}{\left(1+r\right)\sin^2\theta-\overline{\gamma}\sin^2\frac{\pi}{M}}\exp\left[-\frac{r\overline{\gamma}\sin^2\frac{\pi}{M}}{\left(1+r\right)\sin^2\theta-\overline{\gamma}\sin^2\frac{\pi}{M}}\right]. \quad (31)$$

Although this integral cannot be put in a closed form, we are able to carry out the integration in Eq. (31) using a simple 30-point Gaussian-Legendre quadrature formula, which yields high accuracy. It is useful to have a simple closed-form upper bound on the error probability, which can be obtained by simply noting that $\sin^2\theta\le1$. The integral in Eq. (30) is reduced to

$$p_S\left(E\mid\gamma\right)\le\frac{M-1}{M}\exp\left(-\gamma\sin^2\frac{\pi}{M}\right). \quad (32)$$

By using this upper bound along with the PDF of the instantaneous SNR Eq. (28) in the symbol error probability Eq. (29), after some algebra, we obtain an upper bound for the SEP in an M-PSK receiver:

$$p_S\left(E\right)\le\frac{M-1}{M}\ \frac{\left(1+r\right)}{\left(1+r\right)-\overline{\gamma}\sin^2\frac{\pi}{M}}\ \exp\left[-\frac{r\overline{\gamma}\sin^2\frac{\pi}{M}}{\left(1+r\right)+\overline{\gamma}\sin^2\frac{\pi}{M}}\right]. \quad (33)$$

Comparison with the exact result Eq. (31) shows that the upper bound Eq. (33) estimates the SEP with sufficient accuracy to be useful in many practical situations.

Figures 1-3 show the effect of atmospheric turbulence on QPSK with coherent detection using modal-compensated heterodyne or homodyne receivers. We study the SEP Eq. (31) as a function of several parameters: the average turbulence-free SNR γ_0 per symbol, the receiver aperture diameter D, the number of spatial modes J removed by the compensation system, and the strength of atmospheric turbulence. Turbulence is quantified by two parameters: the phase
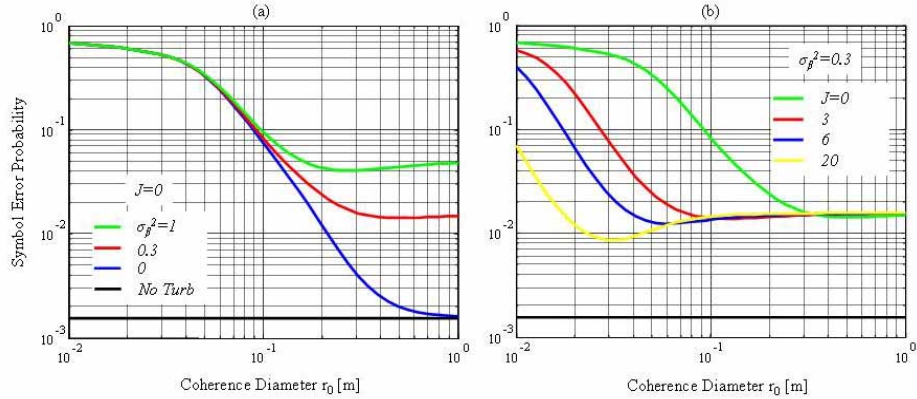
Fig. 2. SEP vs. coherence diameter r_0 for QPSK with coherent detection and AWGN. In (a), no phase compensation is employed, and performance is shown for different values of the scintillation index σ_β^2. In (b), the scintillation index is fixed at $\sigma_\beta^2 = 0.3$, and performance is shown for different values of J, the number of modes corrected by adaptive optics. The severity of atmospheric turbulence increases when r_0 decreases. In all cases, we assume the turbulence-free SNR per symbol is $\gamma_0 = 10$ dB, and the receiver aperture diameter is $D = 10$ cm. In (a), the σ_β^2 ranges from 0.3 (weaker turbulence) to 1 (stronger turbulence). In (b), the compensating phases are expansions through tilt ($J=3$), astigmatism ($J=6$), and 5th-order aberrations ($J=20$). The no-turbulence case is indicated by black lines.

coherence length r_0 and the scintillation index σ_β^2. We consider two nonzero values of the scintillation index. The value $\sigma_\beta^2 = 0.3$ corresponds to relatively low scintillation levels, while $\sigma_\beta^2 = 1$ corresponds to strong scintillation, but still below the saturation regime. When the turbulence reaches the saturation regime, wavefront distortion becomes so severe that it would be unrealistic to consider phase compensation. In most practical free-space links, amplitude fluctuations are not saturated [15].

Figure 1 presents the SEP vs. turbulence-free SNR γ_0. Figure 1(a) shows the performance for different values of the normalized aperture diameter D/r_0, while Fig. 1(b) shows the performance for different values of J, the number of modes compensated. We assume no scintillation, $\sigma_\beta^2=0$, so the effect of turbulence is simply to reduce the coherence length r_0. For a fixed aperture diameter D, as r_0 is reduced, the normalized aperture diameter D/r_0 increases, and turbulence reduces the heterodyne or homodyne downconversion efficiency. Even using a relatively small normalized aperture diameter $D/r_0=1$, turbulence introduces more than a 15-dB performance penalty at 10^{-3} SEP. When phase correction is used, as in Fig. 1(b), in most situations, compensation of just a few modes yields a substantial performance improvement. Compensation of $J = 20$ modes yields significant improvement for even the largest normalized apertures considered. For example, for a normalized aperture $D/r_0=10$, at a SEP = 10^{-3}, the SNR penalty is just over 5 dB. This value should be contrasted with the 15-dB penalty observed in Fig. 1(a) for $D/r_0 = 1$ when $J = 0$, i.e., no modes are compensated.

Figure 2 shows the SEP vs. the phase coherence diameter r_0. Figure 2(a) shows the performance for different values of the scintillation index σ_β^2, while Fig. 2(b) shows the performance for different values of J, the number of modes compensated. In all cases presented, the turbulence-free SNR has a value $\gamma_0 = 10$ dB. The aperture diameter is fixed in every plot to $D = 10$ cm. As we observe in Fig. 2(a), for strong turbulence, corresponding to small values of r_0, the SEP is substantially independent of the scintillation index σ_β^2. In this regime, phase distortions have a large impact, and high-order phase corrections may be required. We note that in this regime of strong turbulence, the coherent part of α^2 is very
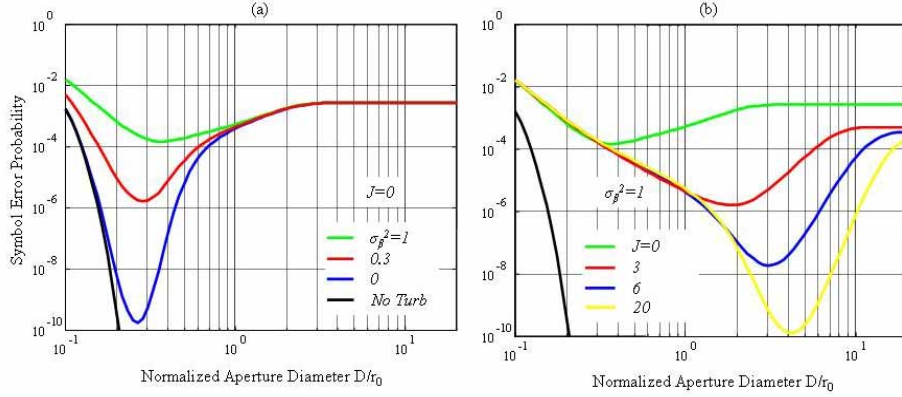
Fig. 3. SEP vs. normalized receiver aperture diameter D/r_0 for QPSK with coherent detection and AWGN. In (a), no phase compensation is employed, and performance is shown for different values of the scintillation index σ_β^2. In (b), the scintillation index is fixed at $\sigma_\beta^2 = 0.3$, and performance is shown for different values of J, the number of modes corrected by adaptive optics. In all cases, the turbulence-free SNR per symbol γ_0 is proportional to the square of the aperture diameter D. For the smallest aperture considered, we assume $\gamma_0 = 10$ dB. In (a), σ_β^2 ranges from 0.3 (weaker turbulence) to 1 (stronger turbulence). In (b), the compensating phases are expansions up to tilt ($J=3$), astigmatism ($J=6$), and 5th-order aberrations ($J=20$). The no-turbulence case is indicated by black lines.

weak, $r \rightarrow 0$, and intensity fading becomes negative-exponential distributed, i.e. $p_\gamma(\gamma) = 1/\overline{\gamma} \exp(-\gamma/\overline{\gamma})$. In this case, SEP Eq. (31) reduces to

$$p_S(E) = \left(\frac{M-1}{M}\right)\left\{1 - \sqrt{\frac{\overline{\gamma}\sin^2\frac{\pi}{M}}{1+\overline{\gamma}\sin^2\frac{\pi}{M}}}\left(\frac{M}{(M-1)\pi}\right)\left[\frac{\pi}{2} + \tan^{-1}\left(\sqrt{\frac{\overline{\gamma}\sin^2\frac{\pi}{M}}{1+\overline{\gamma}\sin^2\frac{\pi}{M}}}\cot\frac{\pi}{M}\right)\right]\right\}. \quad (34)$$

For the strongest turbulence (i.e., smallest r_0) considered, $\overline{\gamma} \rightarrow 0$ and the SEP Eq. (34) asymptotes to a maximum value $(M-1)/M$. In the plots shown, where $M=4$, we have $p_s(E) \rightarrow 3/4$.

Figure 3 considers the effect of aperture diameter on performance. It presents the SEP as a function of the normalized aperture diameter D/r_0 for a constant phase coherence length r_0 and constant scintillation index σ_β^2. For the smallest aperture diameter considered, the turbulence-free SNR has a value $\gamma_0 = 10$ dB. For any other aperture diameter, the value of γ_0 is proportional to D^2. Figure 3 illustrates the concept of an optimal aperture diameter in coherent free-space links. This optimal aperture diameter, which minimizes the SEP, exhibits two different regimes in our studies. For relatively small apertures, amplitude scintillation is dominant, and performance is virtually unaffected by wavefront phase correction. When the aperture is larger, phase distortion becomes dominant, and high-order phase correction may be needed to improve performance to acceptable levels. In [7], the simulation of beam propagation was used to examine the uncertainty inherent to the process of optical power measurement with a practical heterodyne receiver because of the presence of refractive turbulence. Phase-compensated heterodyne receivers were also considered for overcoming the limitations imposed by the atmosphere by the partial correction of turbulence-induced wave-front phase aberrations. As in the current analysis, simulations indicated that the optimal aperture diameters, those minimizing the relative error, separate two different regimes in our simulations. The regime dominated by amplitude scintillation was defined for relatively small apertures and it was virtually unaffected by phase-front corrections. When larger apertures were considered, phase distortion was the relevant effect of turbulence, amplitude fluctuations

were of little influence, and we needed high-order phase corrections to decrease the uncertainty to acceptable levels.

In Fig. 3(a), no phase compensation is employed ($J=0$), and the performance is shown for different values of the scintillation index σ_β^2. Here, the optimal normalized aperture diameter is close to $D/r_0 = 0.3$, and increases slightly with increasing scintillation index. In any case, when σ_β^2 becomes too large, the optimization is of little practical significance. In Fig. 3(b), we consider strong scintillation, $\sigma_\beta^2 = 1$, and show the performance for different values of J, the number of modes compensated. As we increase J, the optimized value of D/r_0 increases, and the optimized SEP improves substantially. Even for such strong scintillation, with compensation of $J = 20$ modes and optimized D/r_0, excellent SEP performance is obtained. In this case, the optimized D/r_0 is rather large (close to 4). For the larger values of D/r_0 considered in these plots, the coherent part of α^2 is very weak ($r \to 0$) and fading intensity becomes negative-exponential-distributed, such that the SEP is described by Eq. (34). In Fig. 3(a), when large normalized apertures D/r_0 are considered, the SEP becomes independent of the scintillation index σ_β^2, and tends toward an asymptotic value that is independent of normalized aperture diameter D/r_0. In Fig. 3(b), at large values of D/r_0, the SEPs also tend toward asymptotic values, independent of normalized aperture diameter D/r_0, which depend only weakly on the scintillation index σ_β^2.

4. Conclusions

We have studied the impact of atmospheric turbulence-induced scintillation and phase aberrations on the performance of free-space optical links in which the receiver uses modal wavefront compensation and synchronous homodyne or heterodyne detection. We have defined a mathematical model for the signal received after propagation through the atmosphere and after modal compensation. By noting that the down converted electrical signal current can be characterized as the sum of many contributions from different coherent regions within the aperture, we showed that the PDF of this signal can be described by a modified Rice distribution. The parameters describing the PDF depend on the turbulence conditions and the number of modes compensated at the receiver. We have provided analytical expressions for the symbol error probability (SEP) for synchronous detection of M-PSK with additive white Gaussian noise, and have used them to study the effect of various parameters on performance, including signal level, aperture diameter, turbulence strength, and the number of modes compensated. We have separately quantified the effects of amplitude fluctuations and wavefront phase distortion on system performance, and have identified two different regimes of turbulence, depending on the receiver aperture diameter normalized to the coherence diameter of the wavefront phase. When the normalized aperture diameter is relatively small, amplitude scintillation dominates and, as phase fluctuations have little impact, performance is virtually independent of the number of modes compensated. When the normalized aperture is larger, amplitude fluctuations become negligible, and phase fluctuations become dominant, so that high-order phase compensation may be needed to improve performance to acceptable levels. We have found that for most typical link designs, wavefront phase fluctuations are the dominant impairment, and compensation of a modest number of modes can reduce performance penalties by several decibels.

Acknowledgment